IEEE Access
Multidisciplinary | Rapid Review | Open Access Journal

Received 13 June 2023, accepted 22 June 2023, date of publication 28 June 2023, date of current version 6 July 2023.

Digital Object Identifier 10.1109/ACCESS.2023.3290160

RESEARCH ARTICLE

Two-Stage Co-Optimization of a Park-Level Integrated Energy System Considering Grid Interaction

LINTAO ZHENG[1,2,3], JING WANG[4], JIONGCONG CHEN[1,2,3], CANTAO YE[1,2,3], AND YULIE GONG[1,2,3]

[1]Guangzhou Institute of Energy Conversion, Chinese Academy of Sciences, Guangzhou 501640, China
[2]Key Laboratory of Renewable Energy, Chinese Academy of Sciences, Guangzhou 501640, China
[3]Guangdong Key Laboratory of New and Renewable Energy Research, Development and Application, Guangzhou 501640, China
[4]Shenzhen Power Supply Bureau Company Ltd., Shenzhen 518020, China

Corresponding author: Cantao Ye (yect@ms.giec.ac.cn)

This work was supported by the Key Science and Technology Project of China Southern Grid Company under Grant 090000KK52220020.

ABSTRACT Park-level integrated energy system has the potential to improve system efficiency and facilitate friendly interaction with the power grid. This paper proposes an integrated energy system for parks that harnesses wind, solar, and geothermal energy sources, alongside three types of energy storage: cold, heat, and electricity. A two-stage coordinated optimization method is proposed that considers both long-term system operation and short-term operation scheduling. The effectiveness of this method is compared with an actual case in Tianjin, and the results demonstrate that the capacity configuration optimized by the two-stage optimization method yields economic and energy-saving benefits under long-term operation. It also satisfies the requirement of near-zero external power load fluctuation or participates in peak shaving and valley filling on the grid side during operation. The proposed two-stage optimization method achieves optimal capacity under long-term operation and favorable interaction with the power grid during daytime scheduling, thereby reducing decision-making difficulties.

INDEX TERMS Integrated energy system, capacity configuration, energy storage, renewable energy.

I. INTRODUCTION

The energy crisis and environmental pollution are pressing issues that countries around the world are facing. Building energy consumption accounts for over one-third of total societal energy consumption and is expected to rise to 50% by 2060 [1] due to development and economic growth. It is of paramount importance to develop comprehensive energy conservation and emission reduction strategies. While an efficient building energy system is undoubtedly one of the pivotal measures to curtail building energy consumption, the current separation of planning, construction, and operation in building energy systems leads to low overall energy conversion efficiency. Therefore, the park-level integrated energy system (PLIES) leverages the complementary characteristics of energy sources to break down various energy network barriers and achieve the coordinated and efficient supply of cooling, heating, and electricity in buildings [2], which is also a hot topic in current energy system research fields [3]. Given the further development of the concept of carbon neutrality and the large-scale increase in renewable energy, the use of PLIES with renewable energy and multi-energy complementarity holds significant implications for energy conservation and emission reduction.

Planning and design are fundamental components of an integrated energy system, with direct impacts on the economy, environment, and system reliability [4]. The planning and design phase must consider the intermittent, flexible, and ever-changing combinations of renewable energy sources and system operation control strategies. Due to this, traditional deterministic optimization methods are insufficient for capacity planning in this context, as observed in [5]. Effective

The associate editor coordinating the review of this manuscript and approving it for publication was Branislav Hredzak.

capacity planning for PLIES can improve system energy supply reliability, meet users' energy quality requirements, and fulfill government environmental protection objectives. The research on system capacity planning is currently limited and mainly centers on minimizing economic costs and environmental costs in micro-grid and distributed power supply capacity planning. However, it is important to pay attention to the size of energy storage devices to balance and optimize IES operation and enable friendly interaction with the power grid. As a high-power consumer in the park, the operation and scheduling of PLIES have a significant impact on the power grid. Therefore, it is crucial to consider the interaction between PLIES in the park and the power grid, which is rarely mentioned in the previous research. To address this research gap, a two-stage optimization method for PLIES that takes into account both economic and environmental factors while ensuring grid compatibility is proposed.

Planning and design constitute crucial technical systems for PLIES, with significant impacts on its economy, reliability, and environmental protection. With the advancements in intelligent algorithms, various optimization algorithms such as the artificial bee colony [6], grasshopper optimization algorithm [7], gray wolf optimization algorithm [8], bat search algorithm [9], firefly algorithm [10], as well as multi-objective algorithms like multi-objective genetic algorithm [11], [12], Non-dominated Sorting Genetic Algorithm II (NSGA-II) [13], and Multi-Objective Particle Swarm Optimization (MOPSO) [14], have found extensive application in optimizing the capacity configuration of PLIES. However, present research has mainly focused on capacity planning for combined heat and power systems, and micro-grids, with some studies only examining the system's economic costs. Even when multi-objective optimization is employed, it typically emphasizes either planning or operational objectives exclusively. Furthermore, most of the current studies have failed to incorporate the interaction capability with the power grid during the operational phase.

To address both planning and operational objectives, numerous studies have proposed a two-stage stochastic optimization method. This approach builds upon the single-stage planning study discussed above and has been extensively applied in various fields, as evidenced by the use of this method in several studies [18], [19], [20], [21], [22], [23], [24], [25]. Typically, the two-stage optimization of integrated energy system (IES) considers the equipment configuration layer in the first stage, while the system operation layer is considered in the other stage. Zhou et al. [23] proposed a two-stage stochastic model that uses genetic algorithms to search for variables in the first stage and Monte Carlo methods in the second stage to handle uncertainty and solve optimization problems. Guo et al. [26] proposed a two-layer collaborative optimization method that considers both the configuration of the upper equipment and the operating parameters of the lower energy storage, which makes the operation of IES more stable and safe. However, hierarchical optimization cannot fully consider the long-term time scale during the operation stage, resulting in most current hierarchical collaborative optimization studies using multiple typical days for analysis. This limitation leads to IES configurations that do not fully consider the impact of seasonal load fluctuations on the operating results. Indeed, the consideration of time scales is crucial in the optimization of IES, and the selection of time scales varies depending on the different optimization objectives. Short-term time scales of 24 hours are typically used when optimizing for operation strategies under fixed designs, while longer time scales are necessary for system planning and design to account for seasonal weather changes and long-term terminal load changes, resulting in more robust solutions [27].

NOMENCLATURE

EST	Energy storage tank.
GSHP	Ground source heat pump.
IES	Integrated energy system.
LCIC	Initial investment of the system's life cycle.
LCOC	Operating cost of the life cycle.
Li-ion	Lithium.
OC	Operating cost.
PV	Photovoltaic.
PLIES	Park-level integrated energy system.
REP	Utilization rate of renewable energy.
SD	Standard deviation.
WT	Wind turbine.
COP_{nom}	Cooling or heating efficiency of the GSHP under full load conditions.
COP_{PLR}	Corrected heat pump efficiency under partial load conditions.
C_i	Initial investment cost of each component of the energy system.
E_b	Rated capacity of Li-ion batter.
E_{user}	Users' electrical load.
$E_{grid-buy}$	Electricity purchased from the power grid.
$E_{grid-waste}$	Waster power of in the renewable system.
E_{grid}	Local peak and valley electricity price.
f	Derating factor of PV panels.
$f_{tank,in}$/ $f_{tank,out}$	Energy storage efficiency/energy release efficiency.
G_{STC}	Light intensity under standard test conditions.
G_{AC} (t)	Light intensity at time t.
N_{PV}	Number of PV panels.
N_{WT}	Number of WTs.
N_{HP}	Number of GSHPs.
P_{STC}	Rated capacity of PV panel.
P_{WT}	Output power of WTs.
P_{r}	Rated power of a WT.

PLR	Part load rate.
$P_{battery,in}$ / $P_{battery,out}$	Charging power of Li-ion batteries/ the discharging power of Li-ion batteries.
$P_{tank,in}$ /$P_{tank,out}$	Charge power of the EST / energy release power of the EST.
Q_{HP-SH}	Heat produced by the GSHP.
Q_{HP-SC}	Cooling capacity of the GSHP.
Q_{h-user}	Users' heating load.
Q_{c-user}	Users' cooling load.
$Q_{tank}(t)$	Cooling capacity or heat storage at time t.
$Q_{tank,max}$	Rated capacity of the EST.
$SOC\ (t)$	State of the battery at the moment.
SOC_{min} / SOC_{max}	Minimum and maximum depth of charge and discharge.
v_i	Starting wind speed of WT.
v_r	Rated wind speed of WT.
v_c	Cut-off wind speed of WT.
W_{HP}	Power consumption of the GSHP.
y	Number of years in the whole life cycle ($y = 60$).

Different optimization objectives can significantly impact the results in IES optimization. The most common objective functions used in capacity configuration optimization are economic, reliability, and environmental indicators. Economic indicators include total operation cost (TOC) [15], total present cost (TPC) [15], [25], [28], and life cycle cost (LCC) [10], [15]. Reliability indicators include on-site load cover ratio [29], [30], deficiency of power supply probability (DPSP) [31], system interactive power [14], [16], load dissatisfaction rate [32], renewable energy penetration [14], and loss of power supply probability (LPSP) [10], [33], [34]. Environmental indicators mainly focus on greenhouse gas emissions, with CO_2 emissions being the most commonly used optimization target [16], [35], [36], [37]. With the increasing promotion and application of renewable energy, the proportion of renewable energy output has become an essential indicator to measure the sustainability of the energy system [15], as it can accurately reflect the actual contribution of renewable energy. Therefore, this study aims to include renewable energy utilization rate (REP) as one of the optimization objectives.

To avoid any potential influence of weight size on the optimization results and to ensure a more robust analysis and decision-making process, this study uses a more rigorous capacity configuration method for PLIES compared to the previous method of determining optimal capacity through TOPSIS or multi-criteria decision-making. It considers factors such as the economy, environment, and the ability to interact with the power grid, and aims to develop an optimal planning and design method which focuses on realizing the interaction between the park and the power grid. In light of PLIES' various renewable energy and energy storage systems, a two-stage optimization mathematical model has been established to determine the optimal capacity configuration. The first stage focuses on optimizing the system capacity configuration over a long timescale. The second stage then filters the capacity configuration obtained in the first stage through optimization over a short timescale to determine the optimal capacity for long-term operation and daytime scheduling, which facilitates good interaction with the power grid and reducing decision-making difficulty. This paper's key contributions can be outlined as follows:

1) An optimization model is developed in two stages, consisting of capacity planning and operation optimization. The first stage involves capacity configuration optimization, which has a significant impact on the objectives and constraints of the second stage's operation optimization. The second stage screens the results of the first stage and determines the optimal capacity configuration. This determination considers the diverse objectives of interaction with the power grid.
2) The first stage in planning the system's capacity involves considering the objective functions of the life cycle initial investment cost (LCIC), life cycle operating cost (LCOC), and REP. This is followed by establishing a PLIES multi-objective capacity planning model that takes into account the impact of electricity, heat, and stepped electricity prices on the system's capacity planning. MOPSO is used to solve the capacity configuration solution set under a typical operating strategy throughout the year.
3) In the second stage of operation optimization, the objective functions are to minimize the external power load fluctuation or participates in peak shaving and valley filling on the grid side. A PLIES operation optimization model is established, which comprehensively considers the interaction capabilities of the park and the power grid. To obtain the optimal system operation solution, a mixed integer linear programming problem (MILP) is solved.

The article is organized as follows: Section II describes the system composition and principle of PLIES used in this study, and briefly describes the control strategy used by PLIES in the first stage of optimization. Section III defines the mathematical model of the main equipment in PLIES. The two-stage co-optimization method and optimization process are introduced in detail in the section IV. Section V conducts a case study to verify the feasibility of the two-stage collaborative optimization method proposed in this study and evaluate the energy-saving potential of the optimized PLIES. Section VI presents significant conclusions that help readers gain a deeper understanding of our research's content.

II. SYSTEM DESCRIPTION

Combined cooling, heating and power supply (CCHP) is the most typical form of IES [38] and has been proven to be an effective solution for energy conservation and emission reduction [39]. However, with the growing promotion of

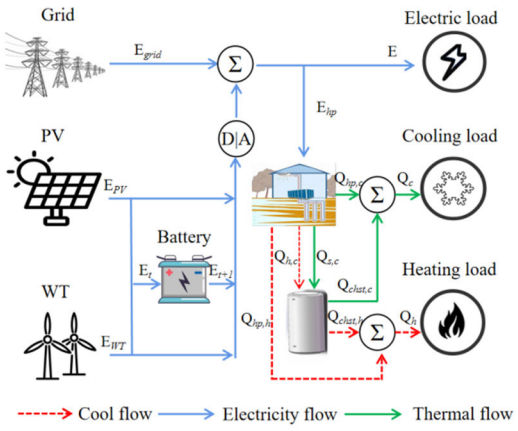

FIGURE 1. Schematic diagram of PLIES.

building electrification, electric energy is increasingly used instead of fossil energy [40], resulting in a reduced application of steam turbines in practical engineering. Therefore, the PLIES proposed in this paper is primarily composed of wind turbines (WTs), Photovoltaic (PV) panels, ground source heat pumps (GSHPs), batteries, energy storage tanks, and the power grid, without consideration of diesel generators or turbine generators, as shown in Fig.1.

PV power generation, WT power generation, batteries and the power grid are combined to satisfy the power demands of energy system and buildings while GSHPs provide users with cold and heat to meet dynamic cooling and heating loads. Additionally, the energy storage tank can effectively adapts the system by storing excess cold and heat under different operating conditions. The batteries are used to improve the system's renewable energy consumption capacity and form a positive interaction with the power grid.

The control of PLIES in this study mainly follows the following principles:

1. The electricity generated by PV panels and WTs is first allocated to meet the electricity demand of users in order to increase the consumption and absorption capacity of renewable energy. If the instantaneous electrical energy generated by PV panels and WTs exceeds the electricity demand, the surplus electricity is stored in the battery. If the battery's maximum capacity is exceeded, the excess electricity is fed into the power grid.

2. Since most of the GSHP units have only fixed frequency operation, an operation strategy is formulated for adding and subtracting units to ensure that the system operates efficiently within the efficiency range of 80-100% load.

3. When the electricity demand cannot be met by PV panels and WTs, the batteries are used first for discharging. If the battery capacity is insufficient, the power grid is used as a backup source to make up for the shortfall in electricity.

4. During periods of low electricity prices at night, the system stores cooling and heating energy by activating the GSHPs and energy storage tank. During periods of high electricity prices during the daytime peak, the energy storage tank is prioritized for the release of cooling or heating. If the stored cooling and heating energy is not sufficient to meet the demand, the GSHPs will be turned on to supplement the shortfall. This operating strategy is commonly used in practical projects.

III. METHODS

A. SYSTEM MATHEMATICAL MODELS

1) RENEWABLE ENERGY GENERATORS

In this study, PV panels and WTs are selected as the renewable energy source equipment, taking advantage of the complementary nature of solar and wind energy. Previous studies have demonstrated that solar and wind energy complement each other to some extent, and their combination can increase the stability of a hybrid system [41], [42], [43]. The power output of PV panels can be calculated using (1) [44], [45].

$$P_{PV}(t) = N_{PV} P_{STC} f \left(\frac{G_{AC}(t)}{G_{STC}}\right)[1 + 0.005 \times (T_t - 25)] \tag{1}$$

where, N_{PV} is the number of PV panels; P_{STC} is the rated capacity, which is taken to be 0.2 kW; f is the derating factor, which is set at 0.95; G_{STC} is the light intensity under standard test conditions, which is taken to be 1 kW/m^2; $G_{AC}(t)$ is the light intensity at time t, Lux; T_t is the ambient temperature, °C.

After obtaining the wind speed of the fan at a height of h, the relationship between the output power of WT and the wind speed can be obtained as follows [44], [46]:

$$P_{WT}(t) = \begin{cases} 0, & v(t) < v_i or v(t) < v_c \\ \dfrac{N_{WT} P_r \left(v(t)^k - v_i^k\right)}{v_r^k - v_i^k} & v_i \le v(t) \le v_r \\ N_{WT} P_r & v_i \le v(t) \le v_c \end{cases} \tag{2}$$

where, N_{WT} is the number of WTs; $P_{WT}(t)$ is the output power of WTs, kW; P_r is the rated power of the unit, 30 kW; v_i refers to the starting wind speed, taking 2.5 m/s; v_r refers to the rated wind speed, which is set to 12 m/s; v_c is the cut-off wind speed, 25 m/s; k is the distribution parameter, which set at 3.

2) ENERGY CONVERSION EQUIPMENT MODEL

The energy conversion equipment involved in this study is the GSHP. GSHP systems can be divided into three types based on the form of geothermal energy exchange: buried pipe GSHP, groundwater GSHP, and surface water GSHP. In this study, a buried pipe GSHP with a 200 m vertical depth is selected. During the cooling season, the GSHP absorbs indoor heat and stores it in the shallow soil through buried pipes, achieving the cooling effect. During the heating season, the buried pipe first extracts heat from the shallow soil,

provides it to the heat pump on the evaporation side of the GSHP, and then converts it into high-grade heat through the GSHP to heat the room. It can be assumed that the heat extracted by the GSHP during the heating season is equivalent to the heat stored in the soil during the cooling season, which constitutes long-term cross-seasonal energy storage. Most existing studies consider the *COP* of the GSHP as a constant value, which is inconsistent with reality [47]. As the GSHP selected in this paper works at full load, the heat production, cooling capacity, and power consumption of the heat pump are calculated using (3)-(5), which are based on the manufacturer's testing data.

$$\begin{aligned} Q_{HP-SH} &= 1434.45 + 48.21T_e - 11.31T_k + 0.78T_e^2 \\ &\quad - 0.057T_eT_k - 0.0126T_k^2 + 0.0045 \end{aligned} \tag{3}$$

$$\begin{aligned} Q_{HP-SC} &= 1199.16 + 40.32T_e - 9.45T_k + 0.66T_e^2 \\ &\quad - 0.048T_eT_k + 0.0105T_k^2 + 0.0045T_e^3 \end{aligned} \tag{4}$$

$$\begin{aligned} W_{HP} &= 229.62 + 8.58T_e - 5.67T_k + 0.129T_e^2 \\ &\quad - 0.327T_eT_k + 0.165T_k^2 + 0.00102T_e^3 \end{aligned} \tag{5}$$

where, Q_{HP-SH} is the heat produced by the GSHP, kW; Q_{HP-SC} is the cooling capacity of the GSHP, kW; W_{HP} is the power consumption of the GSHP, kW; T_e and T_k are the evaporation temperature and condensation temperature, respectively, which are determined according to the soil temperature and the water supply temperature, °C.

The *COP* of the GSHP in the cooling and heating condition are determined:

$$COP_{nom} = \begin{cases} Q_{HP-SC}/W_{HP} & \text{When in cooling condition} \\ Q_{HP-SH}/W_{HP} & \text{When in heating condition} \end{cases} \tag{6}$$

where COP_{nom} is the cooling or heating efficiency of the GSHP under full load conditions.

The selected compressor starts for stepless adjustment as the load reaches 30% of the full load. The *COP* correction of the GSHP with different load rates is calculated:

$$\begin{aligned} &\frac{COP_{PLR}}{COP_{nom}} \\ &= 0.7626 + 0.0017PLR^5 - 0.0181PLR^4 + 0.096PLR^3 \\ &\quad - 0.2697PLR^2 + 0.4276PLR \end{aligned} \tag{7}$$

where, *PLR* is the part load rate; COP_{PLR} is the corrected heat pump efficiency under partial load conditions.

3) ENERGY STORAGE EQUIPMENT MODEL

The energy storage equipment in PLIES proposed in this study includes battery and energy storage tank (EST). Multiple types of energy storage equipment can make rigid power system more flexible, and significantly improving the reliability, safety, flexibility, and economical efficiency of the power grid have been greatly improved [26], [41], [45].

a: BATTERY

The technical performance data used to measure energy storage equipment mainly includes rated power output, charging time, depth of charging and discharging, cycle efficiency, number of cycles, dynamic response time, energy density, and power density [49]. From both technical and economic perspectives, different types of energy storage have their own advantages, disadvantages, and specific usage environments. To achieve the optimal balance between technical and economic factors, the optimal energy storage system configuration may vary depending on specific circumstances. Lithium-ion (Li-ion) batteries are often utilized to store electricity due to the intermittency of renewable energy.

In the first stage, Li-ion batteries are mainly used to ensure the full consumption of renewable energy. When the constraints shown in (8) are met, it is determined that the Li-ion batteries are in a state of charge, and the state of charge at the moment can be calculated by (9).

$$\begin{cases} P_{WT}(t) + P_{PV}(t) > [(1+\beta) \times W_{HP}(t) + E_{user}(t)] \\ SOC\ (t-1) < SOC_{\max} \end{cases} \tag{8}$$

$$SOC\ (t) = (1-\sigma)\, SOC\ (t-1) + P_{battery,in}\ (t)\ \eta_c \Delta t / E_b \tag{9}$$

where, σ is the self-discharge rate of Li-ion batteries which is set at 0.03; $P_{battery,in}$ (t) is the charging power of Li-ion batteries at the moment, kW; η_c is the charging efficiency, which is set at 0.9 [48]; E_b is the rated capacity of Li-ion batteries; E_{user} is the users' electrical load, kW; β is the ratio of the power consumption of the transmission and distribution system and the terminal to that of the GSHP, 30%; $SOC\ (t)$ is the state of the Li-ion battery at the moment, and the initial value of *SOC* is set at 0.8 [26], where $SOC_{\min}$ and $SOC_{\max}$ are the minimum and maximum depth of charge and discharge, respectively.

When the constraints shown in (10) are met, it is determined that the Li-ion batteries are in a discharged state, and the state of charge at the moment can be calculated by (11).

$$\begin{cases} P_{WT}(t) + P_{PV}(t) < [(1+\beta) \times W_{HP}(t) + E_{user}(t)] \\ SOC\ (t-1) > SOC_{\min} \end{cases} \tag{10}$$

$$SOC\ (t) = (1-\sigma)\, SOC\ (t-1) + P_{battery,out}\ (t)\ \Delta t / \eta_d E_b \tag{11}$$

where, $P_{battery,out}$ (t) is the discharging power of Li-ion batteries at the moment, kW; η_d is the discharging efficiency, which is set at 0.9 [50].

In the second stage, Li-ion batteries only need to meet the constraint conditions which are determined by (12)-(13), the charge and discharge state can be adjusted according to the

optimization objectives.

$$\begin{cases} SOC_{\min} \le SOC\ (t) \le SOC_{\max} \\ 0 \le P_{battery,in} \le P_{battery,in,\max} \\ 0 \le P_{battery,out} \le P_{battery,out,\max} \end{cases} \tag{12}$$

$$\begin{cases} P_{battery,in}\ (t) \times P_{battery,out}\ (t) = 0 \\ P_{battery,in}\ (t) \ge 0 \\ P_{battery,out}\ (t) \ge 0 \end{cases} \tag{13}$$

where, the Li-ion battery's maximum charge power, measured in kW, is denoted as $P_{battery,in,\max}$; while its maximum discharge power, also measured in kW, is denoted as $P_{battery,out,\max}$.

b: ENERGY STORAGE TANK

Energy storage tank (EST) can be used to store the heat or cold generated by the energy conversion equipment according to the cooling season and the heating season. Taking the advantages of peak and valley electricity prices, cold and heat storage can be carried out during the low and trough electricity prices at night.

In this study, a simple non-layered water tank model is used. The cooling capacity or heat storage $Q_{tank}\ (t)$ at time t is affected by multiple factors including the cooling capacity or heat storage $Q_{tank}\ (t\text{-}1)$ at time t-1, heat loss coefficient σ_{tank} (which is set to 0.01), rated capacity $Q_{tank,\max}$ in kWh; charge power of the EST $P_{tank,in}$ in kW; energy storage efficiency $f_{tank,in}$ (which is set to 0.92), energy release power $P_{tank,out}$ in kW and energy release efficiency $f_{tank,out}$ (which is set to 0.92). The mathematical model of the EST can be calculated by (14)-(16), and the reliability of the model has been verified experimentally [50].

$$\begin{aligned} Q_{tank}(t) = Q_{tank}(t-1) \times (1-\sigma_{tank}) \\ + \frac{P_{tank,in}\ (t) \times f_{tank,in} \times \Delta t}{3600} \\ - \frac{P_{tank,out}\ (t) \times \Delta t}{f_{tank,out} \times 3600} \end{aligned} \tag{14}$$

$$0 \le Q_{tank}(t) \le Q_{tank,\max} \tag{15}$$

$$\begin{cases} P_{tank,in}\ (t) \times P_{tank,out}\ (t) = 0 \\ P_{tank,in}\ (t) \ge 0 \\ P_{tank,out}\ (t) \ge 0 \end{cases} \tag{16}$$

B. TWO-STAGE CO-OPTIMIZATION METHOD

1) DECISION VARIABLES

a: FIRST STAGE DECISION VARIABLES

Rational capacity configuration plays a crucial role in the economic and energy efficiency of the entire energy system. For instance, if the capacity of the wind power generation system is too large, wind power may not be fully utilized due to its concentration during nighttime when the electricity demand is low. Excess power may then cause severe impact on the power grid or require excessive batteries, which could decrease overall economic efficiency. Similarly, in matching the capacity of energy storage equipment, selecting a capacity that is too large would result in a significant increase in the initial investment, system risk, and potential difficulties in user acceptance. Conversely, a capacity that is too low would hinder the energy storage system's ability to fully realize its adjustment function, thus limiting the advantages of efficient operation of the overall system. Therefore, the number of PV panels (N_{PV}), the number of WTs (N_{WT}), the number of GSHPs (N_{HP}), the rated capacity of EST ($Q_{tank,\max}$), and the rated capacity of Li-ion batteries(E_b) should be selected as decision variables in the first stage.

b: SECOND STAGE DECISION VARIABLES

In addition to considering the optimization of capacity configuration on a long-term timescale, it is also important to focus on the operating performance of different capacity configurations on a short-term timescale. The operating parameters of Li-ion batteries, EST, and GSHPs play a critical role in the overall operation of PLIES, reducing the operating costs of the system and improving interaction with the power grid. Therefore, the hourly status of the PV system, WT system, Li-ion batteries, EST, and GSHPs will be used as decision variables in the second stage.

2) WORK CHARACTERISTIC CONSTRAINTS

To ensure optimal results, the optimization process must comply with both the primary equipment capacity constraints established during the first optimization stage and the energy storage equipment constraints detailed in Section III.These constraints include (1)–(16) and additional constraints specified in (17)–(19). Electrical balance constraints:

$$\begin{aligned} N_{PV} \times P_{PV}\ (t) + N_{WT} \times P_{WT}\ (t) \\ + P_{battery,in}\ (t)\ \eta_c \Delta t + E_{grid-buy}\ (t) \\ = (1+\beta) \times W_{HP}\ (t) + E_{user}\ (t) \\ + E_{grid-waster}\ (t) + P_{battery,out}\ (t)\ {}^{\Delta t}/_{\eta_d} \end{aligned} \tag{17}$$

where, $E_{grid-buy}$ is the electricity purchased from the power grid, kW; $E_{grid-waste}$ is the waster power of in the renewable system, kW. Thermal balance constraints:

$$\begin{aligned} N_{HP} \times Q_{HP-SH}\ (t) \times PLR + P_{tank,out}\ (t) \\ = Q_{h-user}\ (t) + P_{tank,in}\ (t) \end{aligned} \tag{18}$$

where, Q_{h-user} is the users' heating load, kW, and N_{HP} is the number of GSHP in operation. Cold balance constraints:

$$\begin{aligned} N_{HP} \times Q_{HP-SC}\ (t) \times PLR + P_{tank,out}\ (t) \\ = Q_{c-user}\ (t) + P_{tank,in}\ (t) \end{aligned} \tag{19}$$

where, Q_{c-user} is the users' cooling load, kW.

In addition to energy balance, it is necessary to restrict the storage of cold and heat only during the trough of electricity consumption to ensure that the storage of cold and heat is equal to the discharge of cold and heat throughout the day.

3) OBJECTIVE FUNCTIONS

a: FIRST STAGE OBJECTIVE FUNCTIONS

Optimization objectives are diverse based on with different needs and preferences. Initial investment costs, operating costs, renewable energy utilization, and environmental factors are often considered in the optimization of IES. Therefore, LCIC, LCOC,and REP are selected as the objective functions of this study.

LCIC discussed in this paper only includes the purchasing cost of the energy system, which can be calculated from (20).

$$LCIC = \sum_{i=1}^{n} (C_i \times N_i) \tag{20}$$

where, N_i represents the number of components of the energy system; n represents the number of components of the energy system; C_i denotes the initial investment cost, measured in RMB, of each energy system component. The efficient operation of the system through the rational configuration of IES, is critical to reduce operating costs. Therefore, LCOC is selected as one of the objectives in this paper, which can be calculated by (21).

$$LCOC = \sum E_{grid-buy} \times E_{grid} \times y \tag{21}$$

where, E_{grid} is the local peak and valley electricity price, RMB. y is the number of years in the whole life cycle, which is set to 60 according to the typical life of the building.

The wind, solar, and geothermal energy are all considered as renewable energy sources in this study. Among them, the use of GSHP for heating fall within the scope of renewable energy utilization. The "Technical standard for nearly zero energy buildings" GB/T 51350-2019 gives the calculation formula for the REP [51]. As the demand for domestic hot water is not considered in this study, the REP can be calculated by (22).

$$REP = \frac{\sum_{t=1}^{8760} (P_{PV}(t) + P_{WT}(t)) \times 2.6 + \sum_{t=1}^{8760} Q_{HP-SH}(t)}{\sum_{t=1}^{8760} E_{user} \times \delta_c + \sum_{t=1}^{8760} (Q_{h-user}(t) + Q_{c-user}(t))} \tag{22}$$

Here, REP is the proportion of renewable energy output, δ is the proportion of lighting and elevator electricity consumption in total electricity consumption, which is set at 0.5.

b: SECOND STAGE OBJECTIVE FUNCTIONS

Although the capacity configurations of PLIES are determined in the first stage to meet the objectives of LCIC, LCOC, and REP over a long time scale, using PLIES to dispatch energy and achieve good interaction between the park and the power grid is a key issue to be considered in the second stage [52]. Therefore, objective functions are formulated in the second stage based on different interaction methods. The indicators of interaction with the power grid encompass several aspects, including power grid response ability [53], power grid balance ability [53], scheduling and optimization ability [54], [55], reliability [56], and robustness [25]. Based on the focus of this study on evaluating the scheduling capability of PLIES, the first objective function is to reduce the impact on the power grid, which can be expressed as the standard deviation (SD) of the system's external purchased electricity. The external purchased electricity by the entire system should be smoothed as much as possible to achieve good interaction between the park and the power grid. This objective aims to minimize SD and can be calculated by using (23), with a scheduling cycle of 24 hours and a time scale of 1 hour [54].

$$\min SD = \min \left(\sqrt{\frac{1}{24-1} \sum_{t=1}^{24} \left(E_{grid-buy}(t) - \overline{E_{grid-buy}(t)} \right)} \right) \tag{23}$$

where, $\overline{E_{grid-buy}(t)}$ is the average electricity purchased from the power grid.

Another objective function is to adjust the outsourced power load through PLIES, aiming to absorb electricity consumption during the trough of the power grid and reduce it during peak hours. This can help to reduce the peak-to-valley power difference of the grid, promote good interaction between the park and the power grid, and improve the utilization efficiency of the municipal power grid, thereby reducing operating costs (OC) as much as possible [55].

$$\min OC = \min \left(\sum_{t=1}^{24} \left(E_{grid-buy}(t) \times E_{grid}(t) \right) \right) \tag{24}$$

4) OPTIMIZATION METHOD

A two-stage co-optimization method that considers both system configuration and operation strategy is proposed in this study. The proposed method combines the MOPSO, Cplex, and Yamply methods. In the first stage, the optimization problem is transformed into a multi-objective optimization problem, and the Pareto solution set is solved using MOPSO. In the second stage, the optimal solution is selected from the solution set using Cplex and Yamply, which is different from the conventional multi-objective optimization that uses the TOPSIS method for direct selection [24], [28]. As there are conflicts between different objectives, it is not possible to find a solution that satisfies all constraints and objectives in a globally optimal manner. Therefore, the Pareto solution set is obtained using MOPSO in the first stage, which comprehensively considers multiple objectives. The second stage of operation scheduling optimization can be considered as a linear mixed-integer programming problem [44], which can be solved using Cplex and Yamply, which is an interface between MATLAB and Cplex, can be used to integrate the two tools easily [10].

C. OPTIMIZATION SCHEME

The specific optimization process is shown in Fig. 2.

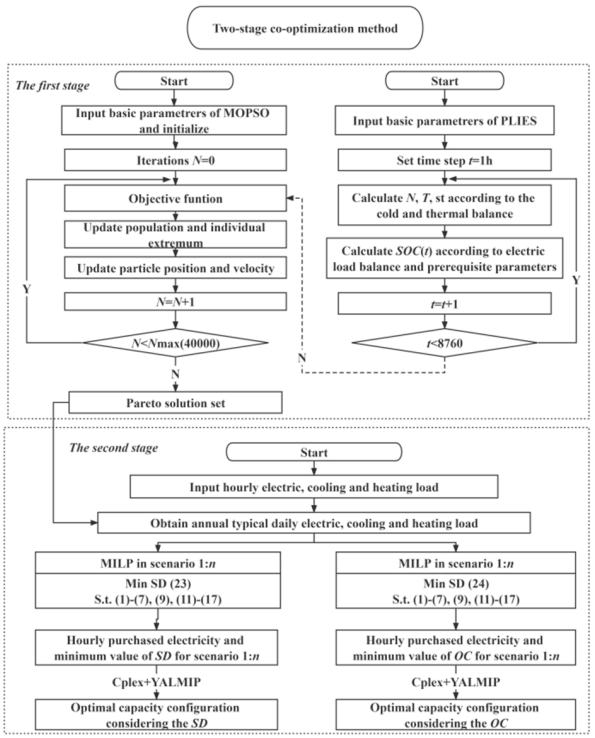

FIGURE 2. Optimization process of the two-stage co-optimization method for PLIES.

Step 1 (Initial Parameter Setting): Local meteorological parameters, the hourly cooling, heating, and electrical load of the park are imported. The relevant parameters and number of iterations of MOPSO are set. The optimization range of N_{WT}, N_{PV}, E_b, N_{HP}, and $Q_{tank,\max}$ are set.

Step 2 (Optimization Model for the First Stage): Based on the parameter settings and constraints established in Step 1, along with the operating strategy outlined in Section II, the hourly system equipment output, and energy consumption of PLIES throughout the year are calculated. As an optimization algorithm, MOPSO is used to obtain a Pareto set that meets the three objectives of LCIC, LCOC, and REP of PLIES.The optimization steps of MOPSO are described in [56].

Step 3 (Optimization Model for the Second Stage): As the Pareto solution set can be obtained from the first stage, the decision-making method is not the conventional TOPSIS or multi-criteria decision-making, but rather screening of the solution set based on the ability to interact with the power grid during the operation stage. Use k-means clustering analysis to obtain the cooling, heating, and electrical load of multiple typical days that capture the annual load characteristics. Then, use all the solutions obtained in the first stage as the input parameters of the second stage. Under the premise of ensuring the energy balance of the system, calculate the equipment output, operating cost, and electricity purchased separately according to the objective function in Eqs.(22)-(23). The capacity configuration solution after effective screening should not only realize good interaction between the park and the power grid but also achieve economical benefits and sustainability, and provide effective guidance for the park's energy planning.

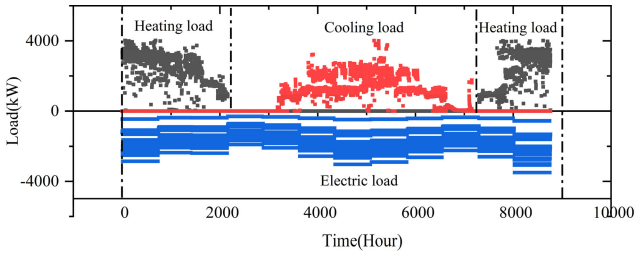

FIGURE 3. Hourly load of the park throughout the year.

IV. CASE STUDY

An office park located in Tianjin, China was used as an example to apply a two-stage co-optimization method for optimizing the capacity configuration of PLIES. The current capacity configuration of the park's PLIES was used as the benchmark to compare the economic feasibility, energy savings, and sustainability of the optimized PLIES.

A. RESEARCH CASE

The selected park in this study comprises of 10 office buildings and 2 dormitory buildings, with a total construction area of 142790 m^2. Fig. 3 shows that hourly cooling, heating, and electrical load were derived from operating data gathered through the energy consumption monitoring system. The annual total cooling load is 4942 MW, with a peak of 4061 kW, while the annual heat load is 7934 MW, with a maximum heat load of 4022 kW. The electrical load remains relatively stable throughout the year, with a maximum of 3489 kW. Renewable energy is mainly provided by the PV system and GSHPs for heating, with the PV system installed on the roof having a capacity of 838.79 kWp. All power generated by the PV system is used on-site, and any excess power is not transferred to the grid. The maximum storage capacity of Li-ion batteries configured in the park is 200 kWh. The park uses three GSHP units as the main heating source, with each unit having a rated heating capacity of 1267 kW and a cooling capacity of 1189 kW. Hourly wind speed and solar radiation for the district are depicted in Fig. 4 and Fig. 5, respectively.

B. SYSTEM PARAMETER SETTING

The electricity prices in Tianjin are presented in Table 1, while Table 2 provides the economic parameters of the equipment. Table 3 shows the parameter settings of MOPSO. When optimizing the capacity configuration of PLIES, practical constraints such as the area available for equipment installation, the amount of renewable energy reserves, and energy security need to be considered. Electrical reliability does not need to be considered in this paper as the required electricity is supplemented by the power grid. The optimal

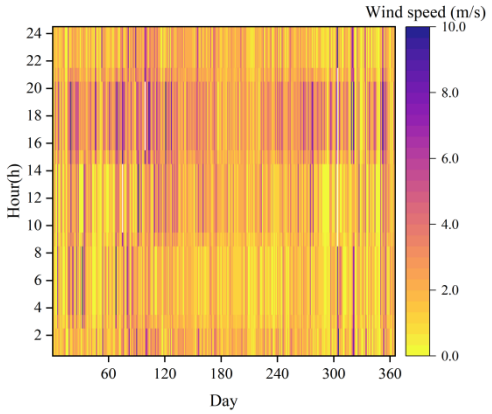

FIGURE 4. Hourly wind speed of the district.

TABLE 1. Electricity prices for different time periods.

Parameter	Unit price (RMB/kWh)	Time period
E_{grid}	0.9175	9:00-12:00; 16:00-21:00
	0.6435	7:00-9:00; 12:00-16:00; 21:00-23:00
	0.3815	23:00-7:00

TABLE 2. Main equipment economic parameters and carbon emission factors [23], [26], [54], [57], [59].

Item	Parameters	Value	Unit
WT	Initial cost	12720	RMB/kW
	Rated Power	3	kW
	Life time	20	Year
	Carbon emissions	957	kg/kW/year
PV panel	Initial cost	4850	RMB/kW
	Rated Power	0.2	kW/pcs
	Life time	25	Year
	Carbon emissions	630	kg/kW/year
GSHP	Initial cost	620	RMB/kW
	Rated Power	1200/1300	kW
	Life time	25	Year
	Carbon emissions	9	kg/kW/year
Geothermal well	Initial cost	1650	RMB/kW
	Carbon emissions	22	kg/kW/year
Li-ion batteries	Initial cost	1400	RMB/kWh
	Rated Power	50	kWh
	Life time	12	Year
	Carbon emissions	17	kg/kWh/year
EST	Initial cost	1000	RMB/m^3
	Life time	20	Year
	Carbon emissions	19	kg/m^3/year

ranges of decision variables in the first stage are determined based on the equipment installation area, cooling and heating load of the park, as indicated in Table 4. The optimal ranges of decision variables in the second stage are mainly determined based on the capacity configuration solution set obtained in the first stage.

TABLE 3. MOPSO parameters in the first stage [14], [17], [59].

Aspect	Item	Symbol	Value
MOPSO	Population number	n	100
	Pareto solution set		100
	Personal and global learning coefficients	c_1,c_2	1.49618
	Inertia weight	w	0.7298
	Inertia weight damping ratio	W_{damp}	0.99
	Maximum iteration number	gen	20000
	Test function		UF10

TABLE 4. Two-stage decision variables.

Aspect	Item	Symbol	Value
Variable search ranges	P_r	P_r (kW)	[0,720]
	N_{pv}	N_{pv} (pcs)	[0,10000]
	E_b	E_b (kWh)	[0,10000]
	N_{HP}	N_{HP} (units)	[0,12]
	$Q_{tank,max}$	$Q_{tank,max}$ (kWh)	[0,25000]

TABLE 5. Test value and calculated value of case.

Aspect	$\sum_{t=1}^{8760}(P_{PV}(t))$ (kWh)	$LCOC$ (RMB)	REP (%)
Test value	948046	8.87×10^8	24.5
Calculated value	1011557	8.58×10^8	25.2

C. MODEL VALIDATION

The accuracy of the mathematical model is crucial for ensuring the reliability of capacity configuration optimization. In this study, the mathematical model described in Section III was used to calculate the total annual PV generation, LCOC, and REP, based on the current park configuration, and the results were compared with the actual operating data. The comparison results are presented in Table 5, which shows a deviation of 6.7%, 3.5%, and 2.8% for total annual PV generation, LCOC, and REP, respectively. These results demonstrate the accuracy of the system mathematical model and the optimization method employed in this study.

V. RESULTS AND DISCUSSION

The analysis of the results of optimizing the capacity configuration in the first stage is presented in Section V-A. Based on the capacity configuration solutions obtained in the first stage, the typical daily operation patterns are introduced in Sections V-B and 5.3, respectively, with the optimization objectives of reducing the impact on the power grid and reducing the system operating cost.

A. PARETO SOLUTION SET OF MULTI-OBJECTIVE OPTIMIZATION IN THE FIRST STAGE

MOPSO is used to obtain the Pareto solution set that satisfies the comprehensive objectives of LCIC, LCOC, and REP. The set contains 100 optimal capacity configuration solutions, as shown in Fig. 6. LCOC and REP decrease significantly

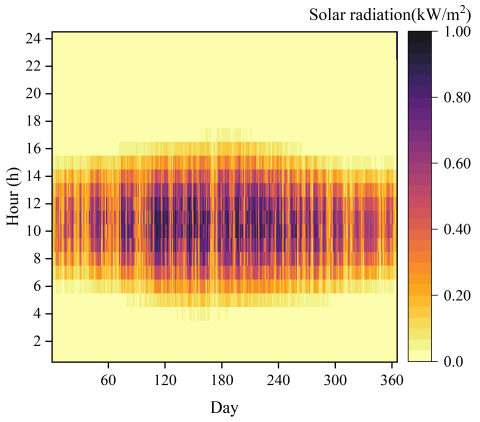

FIGURE 5. Hourly solar radiation of the district.

TABLE 6. The capacity configuration determined by MOPSO method in the first stage.

Aspect	Lower quartile	Median	Upper quartile	Average
P_r (kW)	38	285	460	285
N_{pv} (pcs)	9335	10000	10000	8823
E_b (kWh)	50	622	1306	950
N_{HP} (units)	3	4	5	4
$Q_{tank,\max}$ (m^3)	971	9781	20533	10379
$\Delta LCIC$ ($\times 10^7$ RMB)	0.94	2.6	4.16	2.73
$\Delta LCOC$ ($\times 10^7$ RMB)	-10.37	-9.03	-6.67	-7.85
$\Delta REP(\%)$	16	23	29	21

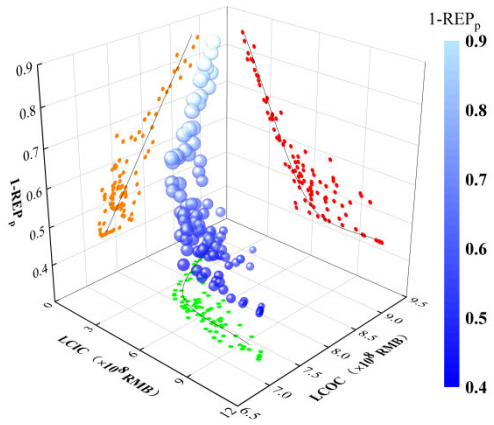

FIGURE 6. The optimal solution set for PLIES capacity configuration in the first stage.

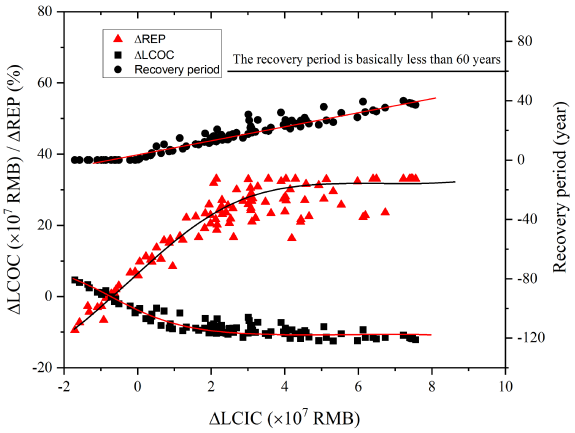

FIGURE 7. The interplay between recovery period, improvement of REP, and the incremental changes in LCOC and LCIC.

as LCIC increases, mainly due to the need to increase the renewable energy equipment. As the capacity of the renewable energy system reaches its maximum, the proportion of heat provided by GSHPs in winter is close to 100%, resulting in the REP also reaching its maximum value after no longer increasing, which is close to 58%.

In the capacity configuration solution set, it is found that the optimal installation number of PV panels is close to the upper limit of the range, with an average value of 8823 pcs, and both the median and upper quantile of the solution set are 10000 pcs. This indicates that the economy and energy-saving performance of the PV system over the entire life cycle are excellent, and the PV panels installed can be increased as much as possible while ensuring the PV generation efficiency. The average and median optimized capacity of WTs in the Pareto solution set is 285 kW, and the upper quantile is only 460 kW, which is below the upper limit. It is recommended to use PV panels as the main power generation and set up WT generation as the auxiliary, which is appropriate. Compared to the current configuration of the park, there are about 1-2 more GSHPs, mainly because in addition to meeting the nighttime load, GSHPs also need to provide energy for thermal storage.

Based on the electricity prices in Tianjin, the maximum recovery cycle range of each capacity configuration in the Pareto solution set can be calculated to be 40 years, with an average of 20 years, which is less than the full lifespan of 60 years. The comparison results with the current capacity configuration of the park are presented in Fig. 7. The reduced LCOC through the optimized capacity configuration in the first stage significantly exceeds the increment of LCIC. Within the payback period, the optimized PLIES through the first stage can reduce LCOC by up to 14.7%, while increasing the *REP* by 33%. Therefore, it can be concluded that the proposed capacity configuration optimization satisfies the requirements of economy and sustainability, and greatly improves the utilization rate of renewable energy.

Although the further increase in the capacity of the EST has not resulted in a significant reduction in LCOC and an increase in REP, it can further enhance the stability of the power grid, which plays a vital role in daytime scheduling. Therefore, the Pareto solution set obtained in the first stage

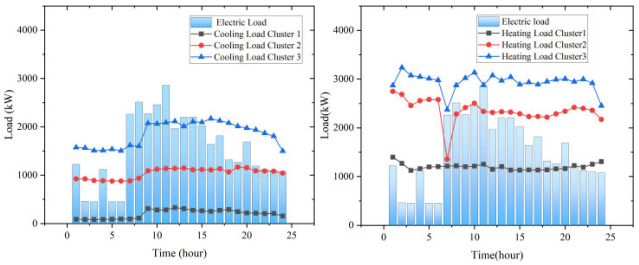

(a) Cooling season (b) Heating season

FIGURE 8. Clustering results of typical daily loads in the park.

TABLE 7. Profile coefficient at different k values.

	k=3	k=4	k=5	k=6	k=7	k=8
Cooling load	0.47	0.39	0.36	0.38	0.38	0.36
Heating load	0.47	0.39	0.41	0.34	0.34	0.37

is further screened by considering the two objectives on the short-term scale in the second stage.

B. SYSTEM OPERATION CHARACTERISTICS

1) GENERATION OF HOURLY LOAD SCENARIOS

Since the second stage's time scale is 24 hours, the park's annual hourly data is clustered using the k-means method to obtain cooling and heating load for multiple typical days. As the value of k has a significant impact on the clustering effect, clustering analysis is conducted with k values of 3, 4, 5, 6, 7, and 8. According to Table 7, the best clustering effect is achieved when k is equal to 3, as the contour coefficient is the highest at this value. It is important to note that the typical daily electrical load is determined by taking the average values of winter and summer, as shown in Fig. 8, as the electrical load changes relatively little.

2) CONSIDER REDUCING EXTERNAL POWER LOAD FLUCTUATION

Due to the high power consumption in the park, a rational PLIES capacity configuration can effectively schedule the electricity consumption in the park and reduce fluctuations in daily purchased electricity, thus improving power grid stability. Fig. 9 shows the daily purchased electricity for six typical days. The capacity configuration obtained from the first stage can reduce fluctuations in daily purchased electricity compared to the current configuration. Multiple capacity configurations can achieve small-scale fluctuations in daily purchased electricity. Therefore, the second stage optimization and screening can obtain superior capacity configurations that not only narrow the scope of decision-making, but also reduce the impact of the park's electricity consumption on the power grid.

Compared with the current park configuration, the capacity configuration obtained in the first stage can reduce the average grid fluctuation rate by 39.5%, 45%, 48.7%, 53.4%,

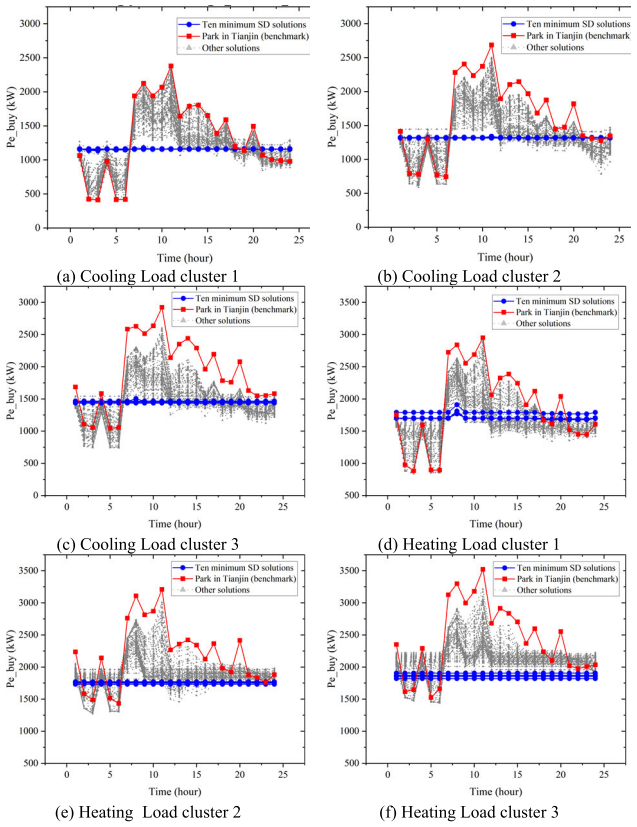

(a) Cooling Load cluster 1 (b) Cooling Load cluster 2
(c) Cooling Load cluster 3 (d) Heating Load cluster 1
(e) Heating Load cluster 2 (f) Heating Load cluster 3

FIGURE 9. Pattern of purchased electricity load for six typical days under the consideration of reducing external power load fluctuation.

63.5%, and 70.9%, respectively, for the six typical days. Some configurations can completely eliminate fluctuations in purchased electricity. The average capacity of the Li-ion batteries and EST in the ten minimum *SD* solutions is 3250 kWh and 19000 kWh, respectively, which is a significant improvement compared to the values in Table 5. Therefore, increasing the capacity of the energy storage system achieves the reduction of daily purchased electricity fluctuations. Li-ion batteries and EST are used to store energy during periods of low electricity consumption and release energy during peak periods.

3) CONSIDER THE EFFECT OF PEAK SHAVING AND VALLEY FILLING

In addition to reducing the impact on the power grid by decreasing fluctuations in purchased electricity, PLIES can also transfer power consumption from peak to off-peak hours through operation scheduling, thereby reducing operating costs and helping to achieve peak shaving and valley filling at the power grid side. Analyzing the objective expressed in (23), the daily operating cost of the capacity configuration in the Pareto solution set is calculated for a typical day. The capacity configuration obtained in the first stage can reduce the daily operating cost range by 14.8-32.3% in six typical days compared to the current park configuration, with Li-ion batteries contributing the most to the cost reduction.

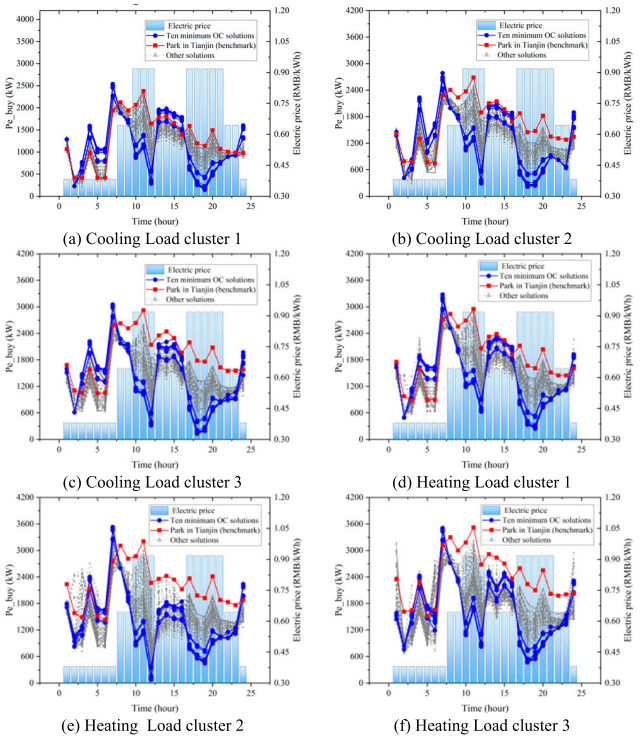

FIGURE 10. Pattern of purchased electricity load for six typical days under the consideration of peak shaving and valley filling in the power grid.

Ten optimal capacity configurations are obtained through the second stage of optimization and screening, and it is found that daily operating costs can be reduced by up to 43.1% in six typical days. It can be concluded that the capacity configuration obtained through the second stage of screening can greatly reduce operating costs.

Fig.10 shows the variation in purchased electricity on six typical days. It can be observed that the optimized capacity configurations can significantly reduce electricity consumption during the two time periods, 9:00-12:00 and 16:00-21:00, compared to the current park configuration. The average capacity of Li-ion batteries and EST in the 10 capacity configurations with the lowest operating cost is 3300 kWh and 22000 kWh, which is similar to the consideration of stable operation. As the capacity of the energy storage system increases, utilizing peak and off-peak electricity prices to reduce operational expenses becomes more advantageous.

4) SOLUTION SET AFTER OPTIMIZATION IN THE SECOND STAGE

After screening for different operating objectives in the second stage, we compared the optimal 10 solutions and found that 8 of them were the same, so we used them as the optimal solution set after screening in the second stage, as shown in Table 8. It can be observed that the configuration of PV panels and WTs are at the upper limit, while the capacity of Li-ion batteries and EST has significantly increased compared to the average value of the capacity configuration solution set in the first stage. This is mainly because, in the actual operation process, it is necessary to adjust the energy storage system according to different operational objectives in order to participate in the interaction with the power grid, which has a significant effect on improving the reliability of the power grid.

TABLE 8. Eight optimal capacity configurations determined through the two-stage collaborative optimization method proposed in this study.

Solution	P_r (kW)	N_{PV} (pcs)	E_b (kWh)	N_{HP} (units)	$Q_{tank,\max}$ (kWh)
1	600	10000	3747	5	13281
2	600	10000	3333	5	20319
3	600	10000	3729	5	21700
4	600	10000	3531	5	21009
5	600	10000	3630	5	21355
6	600	10000	3581	5	21177
7	600	10000	3605	5	21271
8	600	10000	3593	5	21224

By comparing LCIC and LCOC, we found that all solution sets show that LCOC is lower than LCIC, which means that even with the high initial cost of Li-ion batteries and EST, the optimization of the operational scheduling during the operational stage can reduce the operational cost and make it economically feasible. It should be noted that the reduced operational cost is calculated based on the fixed strategy in the long-term scale of the first stage. Through the analysis results of the second stage, we can know that the reduction in operational cost will be lower than the fixed strategy when the strategy changes during the operational stage, which means that the payback period can be further shortened during the operational optimization stage. This observation further supports the notion that, alongside a well-designed capacity configuration, park administrators must enhance their operational capabilities, elevate the level of system intelligence, and maximize the benefits of comprehensive energy systems.

At the same time, the increase in REP has reached about 33%, which indicates that with the increase in the capacity of Li-ion batteries and EST, the increase in GSHP capacity can also ensure that the utilization of renewable energy in the heating system reaches the maximum. Based on the findings of this study, it can be inferred that the proposed two-stage capacity configuration optimization for PLIES can facilitate a mutually beneficial interaction with the power grid, while simultaneously promoting economic and sustainability benefits.

VI. CONCLUSION

This paper proposes the construction of a PLIES consisting of PV panels, WTs, GSHPs, batteries, energy storage tanks, and the power grid. A two-stage capacity configuration optimization method is proposed to investigate the PLIES's operational and economic performance, considering both the system's long-term economic performance and short-term interaction with the power grid. The feasibility and reliability of the proposed two-stage capacity optimization algorithm

are demonstrated through a comprehensive analysis of the system's economic performance, operating characteristics, and energy-saving effects using actual operational data from a park in Tianjin. The proposed capacity optimization model satisfies the comprehensive objectives of life cycle initial investment, life cycle operating costs, and renewable energy utilization rate while also considering the fluctuation of daily purchased electricity load, achieving friendly interaction with the grid, and reducing the impact of the park's large electricity usage on the grid or assisting in peak shaving and valley filling.

Although there has been significant research on the subject, more work is required to establish a coordination mechanism between PLIES capacity planning and system operation. The refinement of mathematical models, optimization of operational algorithms, and the development of high-precision prediction algorithms are crucial for harnessing the benefits of PLIES. However, this study is constrained by the coarse granularity of the monitored case data and the absence of wind power operational data, preventing a thorough validation of all mathematical models. Future efforts will focus on acquiring additional park data to comprehensively verify the proposed methods put forth in this study.

REFERENCES

[1] Z. Liu, G. Fan, D. Sun, D. Wu, J. Guo, S. Zhang, X. Yang, X. Lin, and L. Ai, "A novel distributed energy system combining hybrid energy storage and a multi-objective optimization method for nearly zero-energy communities and buildings," *Energy*, vol. 239, Jan. 2022, Art. no. 122577.

[2] Y. Wang, "A study on the optimization method for integrated energy system operation with multi-objective game theory," *Energy*, vol. 245, 2022.

[3] N. Good, "Using behavioural economic theory in modelling of demand response," *Appl. Energy*, vol. 239, pp. 107–116, Apr. 2019.

[4] M. Wang, J. H. Zheng, Z. Li, and Q. H. Wu, "Multi-attribute decision analysis for optimal design of park-level integrated energy systems based on load characteristics," *Energy*, vol. 254, Sep. 2022, Art. no. 124379.

[5] Y. Wang, "A planning and operation method for regional integrated energy systems that considers both economic and environmental factors," *Energy*, vol. 171, pp. 731–750, Mar. 2019.

[6] S. Singh and S. C. Kaushik, "Optimal sizing of grid integrated hybrid PV-biomass energy system using artificial bee colony algorithm," *IET Renew. Power Gener.*, vol. 10, no. 5, pp. 642–650, May 2016.

[7] A. L. Bukar, C. W. Tan, and K. Y. Lau, "Optimal sizing of an autonomous photovoltaic/wind/battery/diesel generator microgrid using grasshopper optimization algorithm," *Sol. Energy*, vol. 188, pp. 685–696, Aug. 2019.

[8] S. Sharma, S. Bhattacharjee, and A. Bhattacharya, "Grey wolf optimisation for optimal sizing of battery energy storage device to minimise operation cost of microgrid," *IET Gener., Transmiss. Distrib.*, vol. 10, no. 3, pp. 625–637, Feb. 2016.

[9] T. E. Gümüş, S. Emiroglu, and M. A. Yalcin, "Optimal DG allocation and sizing in distribution systems with Thevenin based impedance stability index," *Int. J. Electr. Power Energy Syst.*, vol. 144, Jan. 2023, Art. no. 108555.

[10] M. Shivaie, M. Mokhayeri, M. Kiani-Moghaddam, and A. Ashouri-Zadeh, "A reliability-constrained cost-effective model for optimal sizing of an autonomous hybrid solar/wind/diesel/battery energy system by a modified discrete bat search algorithm," *Sol. Energy*, vol. 189, pp. 344–356, Sep. 2019.

[11] A. Kaabeche, S. Diaf, and R. Ibtiouen, "Firefly-inspired algorithm for optimal sizing of renewable hybrid system considering reliability criteria," *Sol. Energy*, vol. 155, pp. 727–738, Oct. 2017.

[12] A. S. O. Ogunjuyigbe, T. R. Ayodele, and O. A. Akinola, "Optimal allocation and sizing of PV/wind/split-diesel/battery hybrid energy system for minimizing life cycle cost, carbon emission and dump energy of remote residential building," *Appl. Energy*, vol. 171, pp. 153–171, Jun. 2016.

[13] A. Abdelkader, A. Rabeh, D. Mohamed Ali, and J. Mohamed, "Multi-objective genetic algorithm based sizing optimization of a stand-alone wind/PV power supply system with enhanced battery/supercapacitor hybrid energy storage," *Energy*, vol. 163, pp. 351–363, Nov. 2018.

[14] A. Kamjoo, A. Maheri, A. M. Dizqah, and G. A. Putrus, "Multi-objective design under uncertainties of hybrid renewable energy system using NSGA-II and chance constrained programming," *Int. J. Electr. Power Energy Syst.*, vol. 74, pp. 187–194, Jan. 2016.

[15] N. Ghorbani, A. Kasaeian, A. Toopshekan, L. Bahrami, and A. Maghami, "Optimizing a hybrid wind-PV-battery system using GA-PSO and MOPSO for reducing cost and increasing reliability," *Energy*, vol. 154, pp. 581–591, Jul. 2018.

[16] Y. Zhang, H. Sun, J. Tan, Z. Li, W. Hou, and Y. Guo, "Capacity configuration optimization of multi-energy system integrating wind turbine/photovoltaic/hydrogen/battery," *Energy*, vol. 252, Aug. 2022, Art. no. 124046.

[17] J. D. Fonseca, J.-M. Commenge, M. Camargo, L. Falk, and I. D. Gil, "Sustainability analysis for the design of distributed energy systems: A multi-objective optimization approach," *Appl. Energy*, vol. 290, May 2021, Art. no. 116746.

[18] S. Chalil Madathil, E. Yamangil, H. Nagarajan, A. Barnes, R. Bent, S. Backhaus, S. J. Mason, S. Mashayekh, and M. Stadler, "Resilient off-grid microgrids: Capacity planning and N-1 security," *IEEE Trans. Smart Grid*, vol. 9, no. 6, pp. 6511–6521, Nov. 2018.

[19] X. Li, L. Zhang, R. Wang, B. Sun, and W. Xie, "Two-stage robust optimization model for capacity configuration of biogas-solar-wind integrated energy system," *IEEE Trans. Ind. Appl.*, vol. 59, no. 1, pp. 662–675, Jan. 2023.

[20] M. Rahmani, S. H. Hosseinian, and M. Abedi, "Stochastic two-stage reliability-based security constrained unit commitment in smart grid environment," *Sustain. Energy, Grids Netw.*, vol. 22, Jun. 2020, Art. no. 100348.

[21] X. Liu, F. Zhang, Q. Sun, and W. Zhong, "Multi-objective optimization strategy of integrated electric-heat system based on energy storage situation division," *IEEE Access*, vol. 9, pp. 19004–19024, 2021.

[22] X. Xu, X. Jin, H. Jia, X. Yu, and K. Li, "Hierarchical management for integrated community energy systems," *Appl. Energy*, vol. 160, pp. 231–243, Dec. 2015.

[23] Y. M. Al-Humaid, K. A. Khan, M. A. Abdulgalil, and M. Khalid, "Two-stage stochastic optimization of sodium-sulfur energy storage technology in hybrid renewable power systems," *IEEE Access*, vol. 9, pp. 162962–162972, 2021.

[24] Z. Liu, J. Guo, D. Wu, G. Fan, S. Zhang, X. Yang, and H. Ge, "Two-phase collaborative optimization and operation strategy for a new distributed energy system that combines multi-energy storage for a nearly zero energy community," *Energy Convers. Manage.*, vol. 230, Feb. 2021, Art. no. 113800.

[25] R. Yan, J. Wang, S. Lu, Z. Ma, Y. Zhou, L. Zhang, and Y. Cheng, "Multi-objective two-stage adaptive robust planning method for an integrated energy system considering load uncertainty," *Energy Buildings*, vol. 235, Mar. 2021, Art. no. 110741.

[26] Z. Zhou, J. Zhang, P. Liu, Z. Li, M. C. Georgiadis, and E. N. Pistikopoulos, "A two-stage stochastic programming model for the optimal design of distributed energy systems," *Appl. Energy*, vol. 103, pp. 135–144, Mar. 2013.

[27] J. Guo, Z. Liu, X. Wu, D. Wu, S. Zhang, X. Yang, H. Ge, and P. Zhang, "Two-layer co-optimization method for a distributed energy system combining multiple energy storages," *Appl. Energy*, vol. 322, Sep. 2022, Art. no. 119486.

[28] M. André, P. M. Castro, R. M. Lima, and A. Estanqueiro, "Integrated sizing and scheduling of wind/PV/diesel/battery isolated systems," *Renew. Energy*, vol. 83, pp. 1167–1179, Nov. 2015.

[29] R. Li and Y. Yang, "Multi-objective capacity optimization of a hybrid energy system in two-stage stochastic programming framework," *Energy Rep.*, vol. 7, pp. 1837–1846, Nov. 2021.

[30] S. Md, "Cost and exergy-based design optimization of distributed energy systems," *Energy Proc.*, vol. 105, pp. 2451–2459, 2017.
[31] N. Li, "A new outlet for curtailed wind power: Integrated energy systems with CCHP and hydrogen supply," *Appl. Energy*, vol. 303, 2021, Art. no. 117619.
[32] R. Yan, Z. Lu, J. Wang, H. Chen, J. Wang, Y. Yang, and D. Huang, "Stochastic multi-scenario optimization for a hybrid combined cooling, heating and power system considering multi-criteria," *Energy Convers. Manage.*, vol. 233, Apr. 2021, Art. no. 113911.
[33] A. Kaabeche, S. Diaf, and R. Ibtiouen, "Optimal sizing of a renewable hybrid system based on a firefly-inspired algorithm and considering reliability criteria," *Sol. Energy*, vol. 155, pp. 727–738, 2017.
[34] A. Abdelkader, "Sizing optimization of a stand-alone wind/PV power supply system with enhanced battery/supercapacitor hybrid energy storage using multi-objective genetic algorithm," *Energy*, vol. 163, pp. 351–363, 2018.
[35] N. Ghorbani, "GA-PSO and MOPSO-based optimization of a hybrid wind-PV-battery system for cost reduction and reliability improvement," *Energy*, vol. 154, pp. 581–591, 2017.
[36] Y. Chen, Z. Xu, J. Wang, P. D. Lund, Y. Han, and T. Cheng, "Multi-objective optimization of an integrated energy system against energy, supply-demand matching and exergo-environmental cost over the whole life-cycle," *Energy Convers. Manage.*, vol. 254, Feb. 2022, Art. no. 115203.
[37] K. Heine, P. C. Tabares-Velasco, and M. Deru, "Design and dispatch optimization of packaged ice storage systems within a connected community," *Appl. Energy*, vol. 298, Sep. 2021, Art. no. 117147.
[38] Y. Yan, C. Zhang, K. Li, and Z. Wang, "An integrated design for hybrid combined cooling, heating and power system with compressed air energy storage," *Appl. Energy*, vol. 210, pp. 1151–1166, Jan. 2018.
[39] J. Wang, S. You, Y. Zong, H. Cai, and Z. Y. Dong, "Investigation of real-time flexibility of combined heat and power plants in district heating applications," *Appl. Energy*, vol. 237, pp. 196–209, Mar. 2019.
[40] A. Zl, B. Yz, and A. Xw, "Long-term economic planning of combined cooling heating and power systems considering energy storage and demand response," *Appl. Energy*, vol. 279, 2019, Art. no. 114998.
[41] B. Norton, W. B. Gillett, and F. Koninx, "Briefing: Decarbonising buildings in Europe: A briefing paper," *Proc. Inst. Civ. Eng. Energy*, vol. 4, no. 1, pp. 174–183, 2021.
[42] A. A. Solomon, D. M. Kammen, and D. Callaway, "Investigating the impact of wind–solar complementarities on energy storage requirement and the corresponding supply reliability criteria," *Appl. Energy*, vol. 168, pp. 130–145, Apr. 2016.
[43] C. E. Hoicka and I. H. Rowlands, "Solar and wind resource complementarity: Advancing options for renewable electricity integration in Ontario, Canada," *Renew. Energy*, vol. 36, no. 1, pp. 97–107, Jan. 2011.
[44] J. Jurasz, A. Beluco, and F. A. Canales, "The impact of complementarity on power supply reliability of small scale hybrid energy systems," *Energy*, vol. 161, pp. 737–743, Oct. 2018.
[45] T. Ma, J. Wu, L. Hao, W.-J. Lee, H. Yan, and D. Li, "The optimal structure planning and energy management strategies of smart multi energy systems," *Energy*, vol. 160, pp. 122–141, Oct. 2018.
[46] B. Li, R. Roche, D. Paire, and A. Miraoui, "Sizing of a stand-alone microgrid considering electric power, cooling/heating, hydrogen loads and hydrogen storage degradation," *Appl. Energy*, vol. 205, pp. 1244–1259, Nov. 2017.
[47] A. Soroudi, M. Aien, and M. Ehsan, "A probabilistic modeling of photo voltaic modules and wind power generation impact on distribution networks," *IEEE Syst. J.*, vol. 6, no. 2, pp. 254–259, Jun. 2012.
[48] W. Ma, S. Fang, and G. Liu, "Hybrid optimization method and seasonal operation strategy for distributed energy system integrating CCHP, photovoltaic and ground source heat pump," *Energy*, vol. 141, pp. 1439–1455, Dec. 2017.
[49] S. Rehman and A. Z. Sahin, "Wind power utilization for water pumping using small wind turbines in Saudi Arabia: A techno-economical review," *Renew. Sustain. Energy Rev.*, vol. 16, no. 7, pp. 4470–4478, Sep. 2012.
[50] J. Xu, Y. Chen, J. Wang, P. D. Lund, and D. Wang, "Ideal scheme selection of an integrated conventional and renewable energy system combining multi-objective optimization and matching performance analysis," *Energy Convers. Manage.*, vol. 251, Jan. 2022, Art. no. 114989.
[51] T. Bouhal, S. Fertahi, Y. Agrouaz, T. El Rhafiki, T. Kousksou, and A. Jamil, "Numerical modeling and optimization of thermal stratification in solar hot water storage tanks for domestic applications: CFD study," *Sol. Energy*, vol. 157, pp. 441–455, Nov. 2017.
[52] P. Haurdot *Technical Standard for Nearly Zero Energy Buildings*. Beijing, China: China Architecture & Building Press, 2019, p. 39.
[53] R. Pietro, "A multi-agent framework for smart grid simulations: Strategies for power-to-heat flexibility management in residential context," *Sustainable Energy, Grids and Networks*, vol. 34, Jun. 2023, Art. no. 101072.
[54] X. Xu, W. Ming, Y. Zhou, and J. Wu, "Unlock the flexibility of combined heat and power for frequency response by coordinative control with batteries," *IEEE Trans. Ind. Informat.*, vol. 17, no. 5, pp. 3209–3219, May 2021.
[55] C. Cga, "Integrated planning of internet data centers and battery energy storage systems in smart grids," *Appl. Energy*, vol. 281, Jan. 2021, Art. no. 116031.
[56] K. Liu, W. Sheng, S. Wang, H. Ding, and J. Huang, "Stability of distribution network with large-scale PV penetration under off-grid operation," *Energy Rep.*, vol. 9, pp. 1367–1376, Sep. 2023.
[57] H. Li, H.-D. Jiang, K.-Y. Dong, Y.-M. Wei, and H. Liao, "A comparative analysis of the life cycle environmental emissions from wind and coal power: Evidence from China," *J. Cleaner Prod.*, vol. 248, Mar. 2020, Art. no. 119192.
[58] G. Hou, H. Sun, Z. Jiang, Z. Pan, Y. Wang, X. Zhang, Y. Zhao, and Q. Yao, "Life cycle assessment of grid-connected photovoltaic power generation from crystalline silicon solar modules in China," *Appl. Energy*, vol. 164, pp. 882–890, Feb. 2016.
[59] H. Borhanazad, "Optimization of microgrid systems using MOPSO," *Renew Energ*, vol. 71, pp. 295–306, Nov. 2014.

LINTAO ZHENG was born in Guangdong, China, in 1991. He received the B.S. degree in architectural environment and equipment engineering and the M.S. degree in heating, gas supply, ventilation, and air conditioning engineering from Guangzhou University, Guangzhou, China, in 2013 and 2016, respectively, and the Ph.D. degree in building technology science from the South China University of Technology, Guangzhou, in 2019. He is currently a full-time Postdoctoral Fellow with the Guangzhou Institute of Energy Conversion, Chinese Academy of Sciences, Guangzhou. His research interests include integrated energy system optimization, regional energy planning, and air conditioning system optimization.

JING WANG received the M.S. degree in power system and automation from the Huazhong University of Science and Technology, Wuhan, China, in 2012.

She has been involved in researching DC power distribution technology, power grid technology, and flexible resource interaction technology in buildings for a long time.

JIONGCONG CHEN received the M.S. degree in power system automation from the North China Electric Power University, Beijing, China, in 2004, and the Ph.D. degree in power system automation from the South China University of Technology, Guangzhou, China, in 2017. He is currently a Senior Engineer with the Guangzhou Institute of Energy Research, Chinese Academy of Sciences. He has extensive experience in researching related fields, such as power system automation, smart grids, information security, and renewable energy.

CANTAO YE received the B.S. degree in thermal engineering and the M.S. degree in Engineering thermophysics from the South China University of Technology, Guangzhou, China, in 2003 and 2006, respectively. Since 2009, he has been a Senior Engineer with the Guangzhou Institute of Energy Conversion, Chinese Academy of Sciences, Guangzhou. His research interests include distributed renewable energy generation and microgrid technology, and power electronics in distributed power systems.

YULIE GONG received the B.S. and M.S. degrees in thermal energy and power engineering from Tianjin University, Tianjin, China, in 2000 and 2003, respectively, and the Ph.D. degree in thermal energy and power engineering from the Guangzhou Institute of Energy Research, Chinese Academy of Sciences, Guangzhou, China, in 2012.

He is currently a Senior Engineer with the Guangzhou Institute of Energy Research, Chinese Academy of Sciences. He is also a Research Fellow and the Chief of the Geothermal Energy Research Laboratory, Guangzhou Institute of Energy, Chinese Academy of Sciences. Since 2003, he has been conducting scientific research in the laboratory. He has been selected as a member of the Youth Promotion Association of the Chinese Academy of Sciences, a leading talent in the blue industry under Yantai City's "Double Hundred Plan," and a member of the talent team under Zhengzhou City's "1125 Talent Gathering Plan." His research interests include geothermal energy power generation and comprehensive utilization technology, heat pump refrigeration technology, and building energy-saving technology.